A thermography-based method for fatigue behavior evaluation of coupling beam damper

Zhe Zhang
Faculty of Vehicle Engineering and Mechanics Dalian University of Technology, State Key Laboratory of Structural Analysis for Industrial Equipment, Dalian 116024, China

Jinping Ou, Dongsheng Li
Faculty of Infrastructure Engineering Dalian University of Technology, Dalian 116024, China

Shuaifang Zhang
Department of Mechanical Engineering Penn State University, State College 16802, USA

Junling Fan
Aircraft Strength Research Institute, Xi'an 710065, China
fanjunling@mail.dlut.edu.cn

ABSTRACT. Under cyclic load, local fatigue damage will occur in the metal damper widely used in the shear wall. This will deteriorate the stiffness of damper and weaken the hysteresis behaviour. The present paper proposed a new and easy method to manufacture kinds of coupling beam dampers. A thermography-based experiment was used to study the energy dissipation and damage accumulation during fatigue process of the metal damper. Based on the temperature variation related to fatigue damage process, the relationship between the plastic deformation and thermal energy dissipation was quantitatively established. Besides, the relationships between the temperature increase to damage accumulation and mechanical load were analyzed systematically.

KEYWORDS. Coupling beam damper; Hysteresis behavior; Energy dissipation; Fatigue damage.

INTRODUCTION

The coupling shear wall structure is a very common structure type due to its strong anti-lateral stiffness and great load carrying capability. Paulay et al. [1] employed the diagonal crossing reinforcement to improve the seismic resistance of the reinforcement concrete. Coull [2] used the stiffing beam on the top of the shear wall to

strengthen the structure's integrity and improve the lateral stiffness. Fortney et al. [3-4] raised the concept of changeable steel coupling beam, namely safety wire, was weakened to dissipate the energy via shear yielding and could be replaced conveniently after damage. Chung et al. [5] proposed a frictional damping device in the middle of coupling beam to decrease the response of shear wall structure under earthquake. Kim et al. [6,7] developed a compound energy-dissipation damper component by combining high-damp rubber material with two U-Shape Steel plate. Mao et al. [8] proposed a new shape memory alloy damper, which was applied as a replaceable coupling beam.

However, the existing coupling shear beam dampers are very complicate and are difficult for manufacturing. Besides, there is a lack of analysis on the failure mechanism and dissipation performance. Under this background, we proposed an easy-making shear coupling steel beam damper and also designed corresponding cyclic shear experiments to investigate the bearing capacity and energy dissipation performance. Besides, the infrared camera is used during the fatigue test process in order to record the temperature distribution and temperature change. The temperature signal then is used to analyze and evaluate the energy dissipation related to local fatigue damage. Nondestructive evaluation has been used in many areas for a long time, which includes ultrasonic nondestructive testing [9] and Infrared thermography and so on. Based on the temperature variation, infrared thermographic method is applied to determine the fatigue performance parameters in real time [10]. Temperature variation is a macro behavior of energy dissipation during fatigue process, which could reflect the energy transformation during cumulative fatigue damage process and is closely related with the evolution of interior damage [11].

Todhunter [12] studied the relationship between the temperature change and deformation. In the following 160 years, the thermos-elasticity theory was under intensive study and was improved step by step, which has been developed as a systematic theory [13]. Inglis [14] studied the relationship between fatigue and cyclic hysteresis energy, which motivated scholars to study the inner relationship between the damage evolution and the energy absorbption and dissipation during the fatigue process. As the high-speed and high-sensitivity infrared camera came out during the recent 30 years, more and more people not only paid attention on the application of nondestructive testing, but also studied the energy dissipation and thermal energy during the cyclic fatigue test to evaluate the fatigue response based on fatigue damage model and failure criteria [15-17]. Fan et al. [18,19] built the energy relationship of Miner linear cumulative damage theory based on energy dissipation theory and infrared thermography method, which could well predict the residual life of components in an easy understanding way. Zhang [20] and etc designed the coupling beam damper with Kriging surrogate model and provided a new framework to design the coupling beam dampers.

INFRARED THERMOGRAPHY AND ENERGY BALANCE

Introduction to infrared thermography

According to generalized Hooke's law, the stress-strain relationship for isotropic elastic material with thermal load is shown below:

$$\Delta\varepsilon_{ii} = \frac{1-2v}{E}\Delta\sigma_{ii} + 3\alpha\Delta T \tag{1}$$

where, $\Delta\varepsilon_{ii} = \varepsilon_{11} + \varepsilon_{22} + \varepsilon_{33}$ is the change of principle strain, $\Delta\sigma_{ii} = \sigma_{11} + \sigma_{22} + \sigma_{33}$ is the change of principle stress, *a* is the linear expanding coefficient, ΔT is the change of temperature, E is Young's modulus, v is poisson's ratio.

The change of temperature for elastic material under adiabatic condition follows the following rule:

$$\Delta T = -\frac{3\alpha T K \Delta\varepsilon_{ii}}{\rho C_v} \tag{2}$$

In which T is the absolute temperature, C_v is Constant Volume Specific Heat, ρ is density, K is bulk modulus.

By substituting the equation of the relationship between Constant Volume Specific Heat (C_p) and specific heat at constant pressure (C_p): $C_p - C_v = (3E\alpha 2T)/(\rho(1-2v))$, the following equation could be achieved:

$$\Delta T = -\frac{3\alpha T}{\rho C_v}\Delta\sigma_{ii} \tag{3}$$

Which could illustrate that there is a dynamic balance between the mechanical energy and thermal energy under adiabatic condition. The negative sign in this equation shows that the temperature would decrease when the material is under tension while the temperature would increase when the material is under compression. Thermo-elastic effect could not influence the average temperature rise on the sample surface during the fatigue process, it could only affect the temperature around the average temperature periodically, which is in accordance with the period of principle stress with a difference of the phase about 180^0.

Infrared thermography has been widely used in nondestructive testing in many materials and structures in recent years, with the advantage of large detecting area, high speed and non-contact when compared with other nondestructive testing method such as acoustic emission, magnetic-leakage nondestructive examination, X-ray and Eddy Current Testing. The theory of infrared nondestructive testing was firstly built by Carlomagno[21]. For an infinitely large plate ignoring the lateral heat flux diffusion, the heat conduction equation under the periodic heat flux of $q = I_0 e^{jwt}$ with only considering the heat transfer along the direction of thickness is shown below:

$$\frac{\partial T}{\partial t} = \alpha \frac{\partial^2 T}{\partial x^2} \tag{4}$$

$$\text{at} \quad x = 0 : -k\frac{\partial T}{\partial x} = I_0 e^{jwt} \tag{5}$$

In which, T is a function of temperature distribution in space and time, $a = k/(\rho c)$ is the thermal diffusion coefficient, k is the thermal conductivity coefficient, w is angular frequency. Solving this PDE with the separation of variables, the temperature T could be expressed as a function of x and t:

$$T(x,t) = \frac{I_0}{K\sigma} e^{-\sigma x} e^{-jwt} \tag{6}$$

In which $\sigma = \sqrt{jw/a} = (1+j)\sqrt{\frac{2w}{a}} = (1+j)/\mu$, and $\mu = \sqrt{\frac{2a}{w}}$ is the diffusion length, which is also known as the damping coefficient. This equation describes the heat conduction along x under Modulation frequency control.

At least four thermographs in one period must be collected to obtain the phase φ and amplitude A, also Fourier analysis of the thermal image is necessary:

$$\varnothing = arctan\left(\frac{S_3 - S_1}{S_4 - S_2}\right) \tag{7}$$

$$A = \sqrt{(S_3 - S_1)^2 + (S_4 - S_2)^2} \tag{8}$$

Since the thermal properties are different with/without damage under the periodic heat load. Non-uniform heat flux would appear and could result in different temperature amplitudes and phases according to heat conduction theory. Thus the damage could be determined based on this difference.

Infrared thermography experiment method could also monitor the temperature change in real time for structures under cyclic loading so as to find the high stress region and key region of local cumulative fatigue damage. Infrared thermography could provide efficient improvement or maintenance solutions to ensure the safety and reliability. Thus, it is significant to evaluate the safety of structure via Infrared thermography to monitor the local thermal evolution in real time, which not only could ensure the good functioning of structure but also could avoid or reduce the loss due to fatigue damage.

Energy balance during the hysteresis loading proces

Since the elasto-plastic deformation during the fatigue process is irreversible because of cumulative plastic strain energy in aspect of cumulative energy. The thermal energy dissipation evolution is similar with the evolution of temperature field with

damage in structure, so the temperature field during the fatigue process is closely related with the microstructure configuration and its nonlinear interaction with the local damage effect. As a consequence, the fatigue energy dissipation is in accordance with the regularity of thermal energy dissipation, which means that the temperature evolution could reflect the energy dissipation characteristics during the fatigue process. During the fatigue loading process, the mechanical energy, elastic strain energy, plastic energy and anelasticity damping energy are involved. . Specifically, the input energy from outside belongs to mechanical energy, which includes elastic strain energy, plastic strain energy and anelasticity damping energy. Elastic energy corresponds to the recoverable deformation of material crystal, which has no influence on damage accumulation. Anelasticity damping energy is time-related and conditionally reversible, which plays a significant role for high cycle fatigue, but it has very little influence on the total energy dissipation since plastic strain energy is the most important reason that causes damage.

Energy balance law

During the cyclic loading process, most of mechanical energy is dissipated as thermal energy into the surroundings, part of energy will stay in the material and is reflected as the transformation of microstructures. The energy balance law is shown below according to first law of thermodynamics

$$\Delta W(t) = \Delta D(t) + \Delta Q(t) + \Delta E_K(t) + \Delta E_0(t) \tag{9}$$

In which $\Delta W(t)$ is the increment of total input energy during cyclic loading process, $\Delta D(t)$ and $\Delta Q(t)$ are the increment of total storage energy and dissipation energy, respectively, $\Delta E_K(t)$ is increment of kinetic energy, which is zero under cyclic load, $\Delta E_0(t)$ is the energy dissipation increment in other forms, which is relatively very small when compared with $\Delta D(t)$ and $\Delta Q(t)$. Thermal energy dissipation and plastic strain energy during the cyclic loading process will be discussed in the following parts

Characteristics of thermal energy

Most of the mechanical energy will be transferred to thermal energy. This is the typical phenomenon of irreversibility in thermodynamics. Many researches have shown that massive thermal energy would be produced during the fatigue process. The thermal energy dissipation is caused by viscosity or interior friction, which is due to the shear deformation of crystals, specifically. Also, dislocation movement of atoms during the plastic deformation period would convert most energy into thermal energy. Thus, the temperature field caused by fatigue damage evolution will change due to damage distribution and difference of motion for different atoms, also is partially because the thermal energy is different for different material elements. Although the ratio of thermal energy dissipation to total strain energy may be different in different cases, it is certain that thermal energy dissipation is the most important part, which plays a key role during the energy exchange of fatigue process. The thermal energy increment during the cyclic loading is shown below:

$$\Delta Q(t) = \Delta Q_q(t) + \Delta Q_b(t) \tag{10}$$

$$\Delta Q_q(t) = \rho C V \Delta T(t) \tag{11}$$

$$\Delta Q_b(t) = hA\Delta T(t) \tag{12}$$

In which $\Delta Q_q(t)$ is the increment of total interior energy of dampers at time t, $\Delta Q_b(t)$ is the convection thermal energy dissipation at time t, $\Delta T(t)$ is the average temperature rise of dampers, ρ is density, V is the working region volume, C is the specific heat, h is convection coefficient, A is the surface area of damper working zone. This paper assumes that the heat conduction between damper and loading system is negligible, the material of damper is Q235 steel, the material properties are shown in Tab. 1.

ϱ, kg/m³	E, MPa	v	C, Jkg⁻¹K⁻¹	h, $Jm^{-2}s^{-1}K^{-1}$	σ_b, MPa	σ_y, MPa	σ_f, MPa
7860	2.06E5	0.3	504	12.1	406	235	178

Table 1: Physical and mechanical properties of Q235 steel.

Plastic energy accumulation during the cyclic loading

By ignoring the energy dissipation such as acoustic emission, electric and magnetic energy dissipation, then Eq. (9) could be simplified as below:

$$\Delta W(t) = \Delta D(t) + \Delta Q(t) \tag{13}$$

In which $\Delta Q(t)$ is the thermal energy increment, $\Delta D(t)$ could not be got directly but could be achieved by calculating the total energy increment and thermal energy increment.

EXPERIMENTAL DESIGN AND SETUP

Sample description

The sample in this study is a steel plate with two elliptical cutouts both on top and bottom of the plate. The dimension of the sample is 280x160x5 (mm). The centers of these two elliptical holes and the major axis of the ellipse are located on the top and bottom boundary, respectively, as shown in Fig.1. Obviously, the opening area of the holes depends on the opening parameters of a and b, where a is the length of semi-major axis and b the length of minor semi-major axis. The ratio value of a/b is set as a constant of 2, while the opening areas are set different for comparison. As shown in Tab. 2, the opening ratio, defined as the ratio of the opening area to the area of the steel plate, is set as 10%, 15%, 20%, and 25% to get the final optimal opening parameter.

Specimen	Opening ratio	a/mm	b/mm
SPA10	10%	53.42	26.71
SPA15	15%	65.42	32.71
SPA20	20%	75.54	37.77
SPA25	25%	84.46	42.23
SPB10	10%	106.84	53.42
SPB15	15%	130.84	65.42
SPB20	20%	151.08	75.54
SPB25	25%	168.92	84.46

Table 2: Parameters of Shearing couple beam damper.

The samples are made of Q235 steel, with Young's modulus E=2.07e5MPa and poisson's ratio μ=0.3. Tensile test of standard sample selected in the same batch was conducted to find the actual yield strength, the constitutive model achieved in the test is shown in Fig.2.
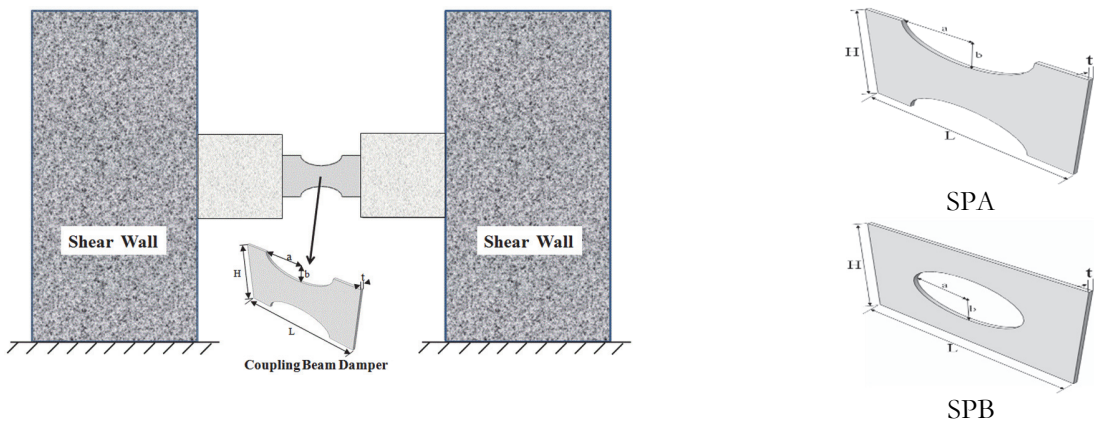

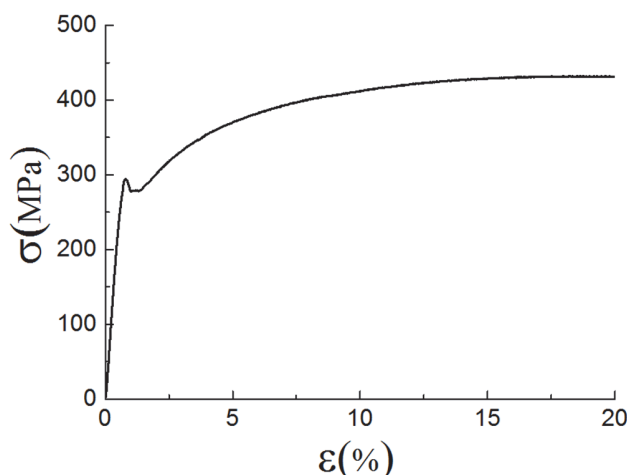Figure 1: Coupling beam damper with top and bottom openings.

Figure 2: Material constitutive curves

Experiment setup

Experiment load and data collection system

The load was applied by MTS material test machine and controlled with displacement load, the curve of which is shown in Fig.3. The time history signal of the actual displacement load and bearing capacity was received by B&K 3050 signal collection system with the software Pulse13.0, where the sample frequency is 1kHz. The data collection system is shown in Fig. 4.
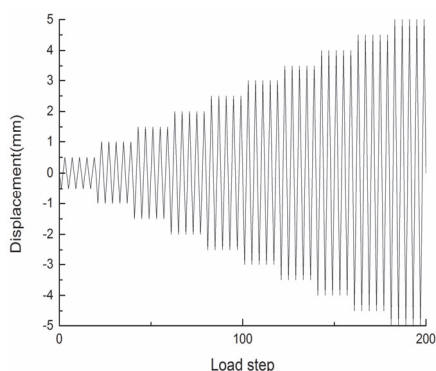

Figure 3: Displacement load curve.

Figure 4: Signal collection system.

Temperature field monitoring system

Another important parameter in this experiment is the temperature field, the Cedip Jade III Infrared camera produced by Cedip company with the technology of infraredfocal plane array was used in this experiment for temperature monitoring and collecting the temperature data. Specifically, the focal plane is composed of 320x240 InSb pixel detectors and could collect the surrounding thermal infrared radiation. The sensitivity of the infrared camera is about 0.001K at the room temperature. The temperature data collection system is shown in Fig.5. Also, the thermo sensitivity is better if the integration time is longer, which is usually set as 1.5ms. The infrared image signal process is based on time-domain averaging method to improve the resolution. Specifically, the random Gaussian noise is reduced via averaging n frames in time-domain to obtain one high quality image, which can be realized by the post-process software ALTAIR. In this experiment, the test sample is fixed with 12 high strength bolts by the sample fixture, which consists of two pairs of asymmetrical L-shape support with the layer width of 20mm, the yield strength of 235MPa and yield strength of 406MPa. Also the two pairs of fixtures are connected and fixed with 20 high-strength bolts so as to fix the sample in the center, and the top and bottom are welded with two symmetrical rod holder with a diameter of Φ 36mm, which is designed for the connection of the fixture and the load experiment system. Also the sample surface is coated with black matted paint to improve the rate of thermal radiation of the sample surface.
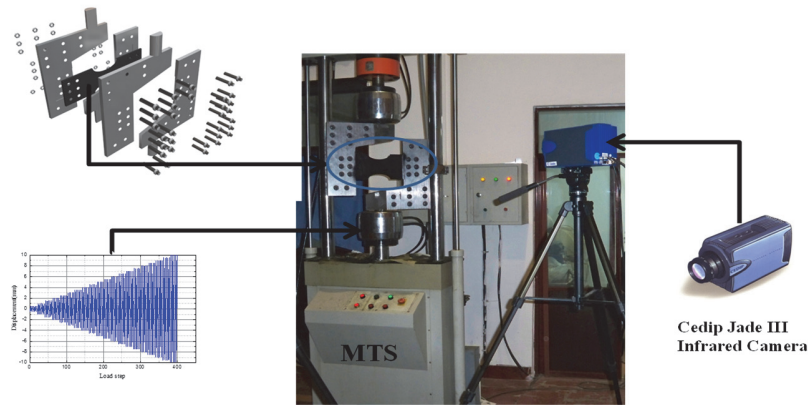
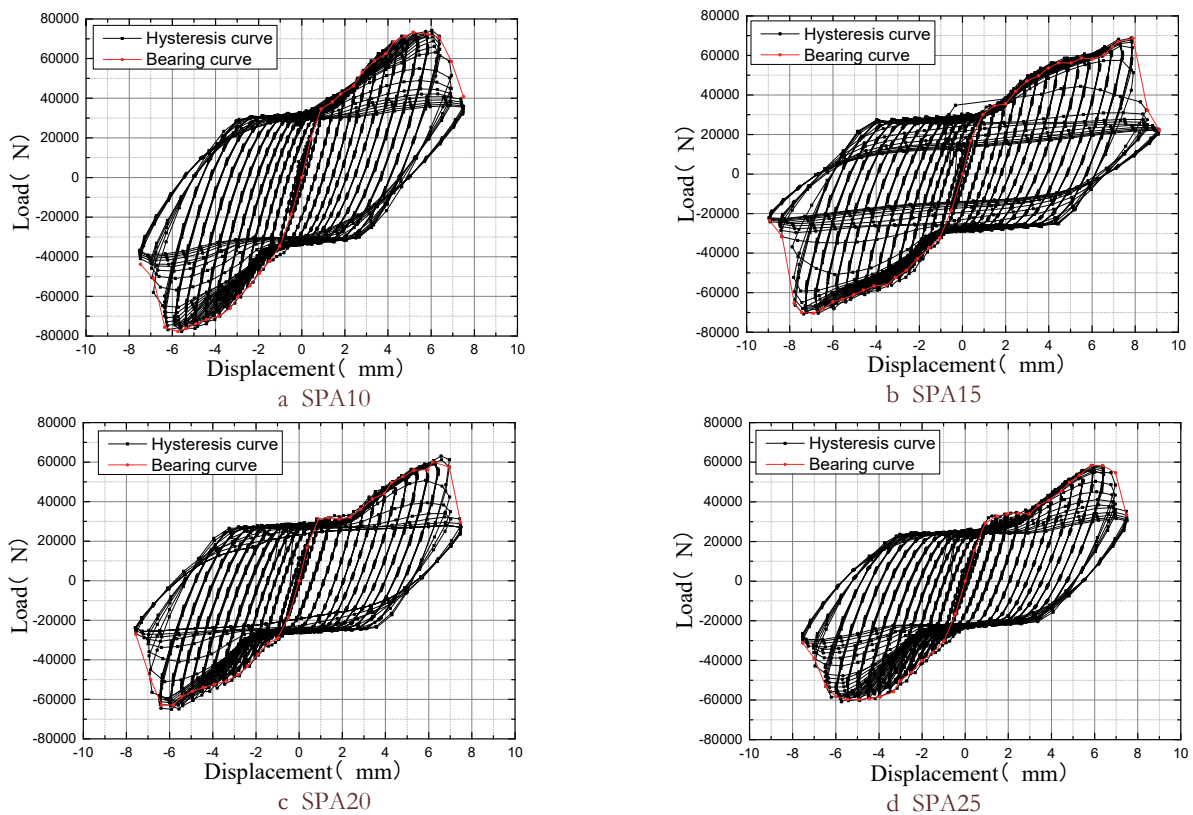Figure 5: Load and temperature monitoring system.

Figure 6: Hysteresis curves of dampers for SPA with different opening ratios.

RESULTS AND DISCUSSION

Hysteretic curve and the skeleton hysteresis curve

The hysteretic curve for a component or a structure is a very important and comprehensive indicator that could represent the earthquake resistance performance as well as a good judgement for structural elasto-plastic analysis. The hysteretic curves for the four different opening ratios are shown in Fig.6, in which SP with displacement load as x-axis and bearing capacity as y-axis. As shown in this figure, all the four curves are very full as well as the stiffness degeneration (cyclic softening) occurs due to damage. Also, by comparing the four curves, we could see that the stress concentration is more and more severe while the maximum bearing capacity is becoming smaller as the opening ratio goes larger. The stiffness degeneration of damper with opening ratio of 25% is minimum in the four tests, which is because of

the high stress concentration and very low bearing capacity of such samples. In general, as the opening ratio becomes larger and larger, the stress concentration near the hole would be larger and the bearing capacity of damper would be smaller. The hysteretic curves of four different opening ratios with centered ellipse openings are shown in Fig.7, which shows that the bearing capacity and ductility would increase as the opening ratio increases. By comparing with Fig.6, we can see that the coupling beam damper with top and bottom opening is much better than the opening type of central opening under the condition of same opening ratio.
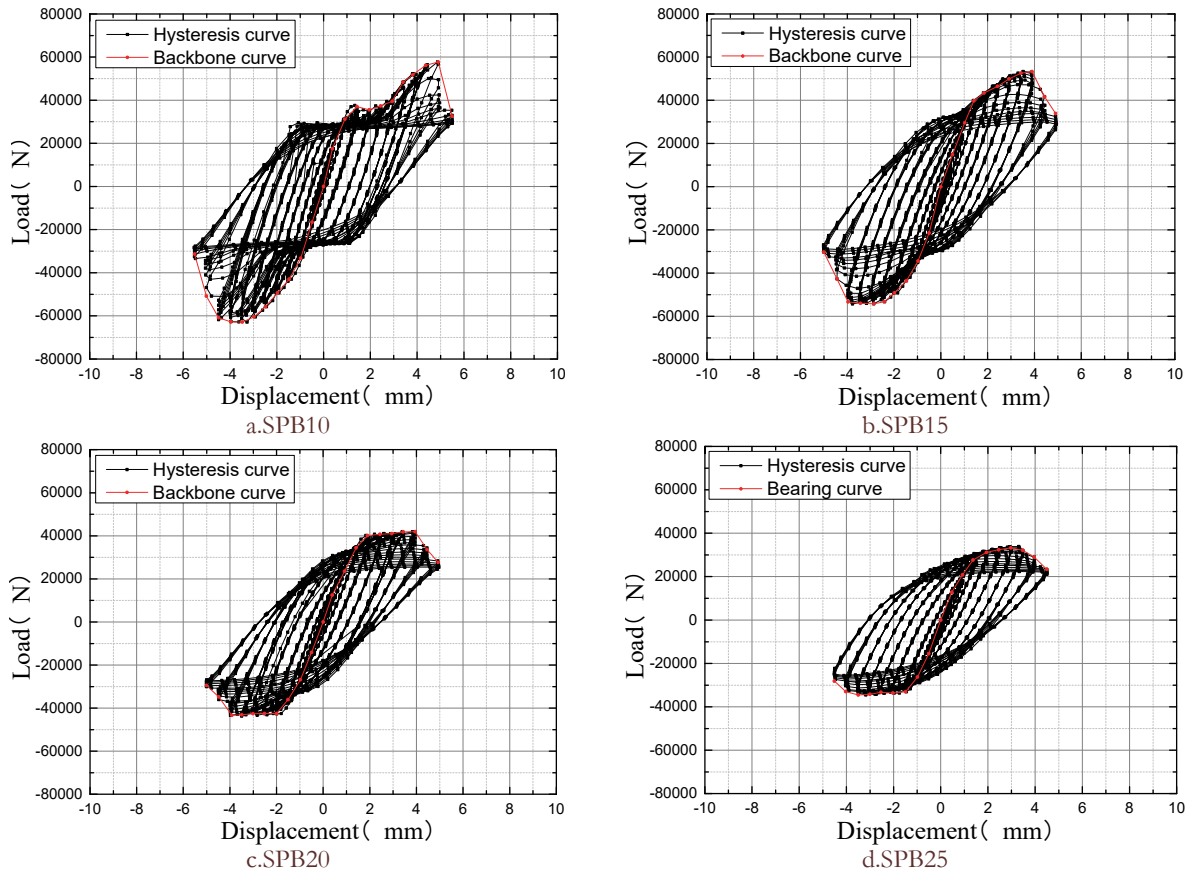

Figure 7: Hysteresis curves of dampers for SPB with different opening ratios.

Cyclic hysteresis energy

It is very important to study the variation rule of stress, strain during the cyclic loading process, the dissipation energy is usually described as the cyclic hysteresis energy, which is the area encircled by the hysteresis curve. Although the plastic deformation is not the only reason that causes the hysteresis phenomenon, which may also be caused by viscoelastic response. But plastic strain energy holds the largest part of the hysteresis energy in low-cycle tests, which means that the plastic strain energy could represent the hysteresis energy with controllable error. As shown in Eq. (14), the hysteresis energy $\Delta W(t)$ represents irreversible plastic energy during each loading and unloading cycle, which is calculated by the area surrounded by the cyclic hysteresis circle.

$$\Delta W(t) = \oint \sigma : d\varepsilon \tag{14}$$

As shown in Fig.8, the cyclic hysteresis energy under the same displacement is smaller as opening ratio becomes larger. As the displacement load goes to 7.5mm, the cumulative dissipation energy of SPA15 exceeds the cumulative energy of SPA10, which is because the plastic deformation of SPA15 is too large so as to make the stiffness degenerate late. As shown in Fig.9, SP15 performs very good hysteresis dissipation capacity. However, the accumulative dissipation energy of SPB with the opening ratio of 15% at the displacement amplitude of 4.5mm is similar with, but did not exceed SPB10

(opening ratio of 10%). As shown in Fig. 8, the dissipation energy of SPA would increase as the opening ratio decreases, which also shows that the energy dissipation performance is much better than SPB.
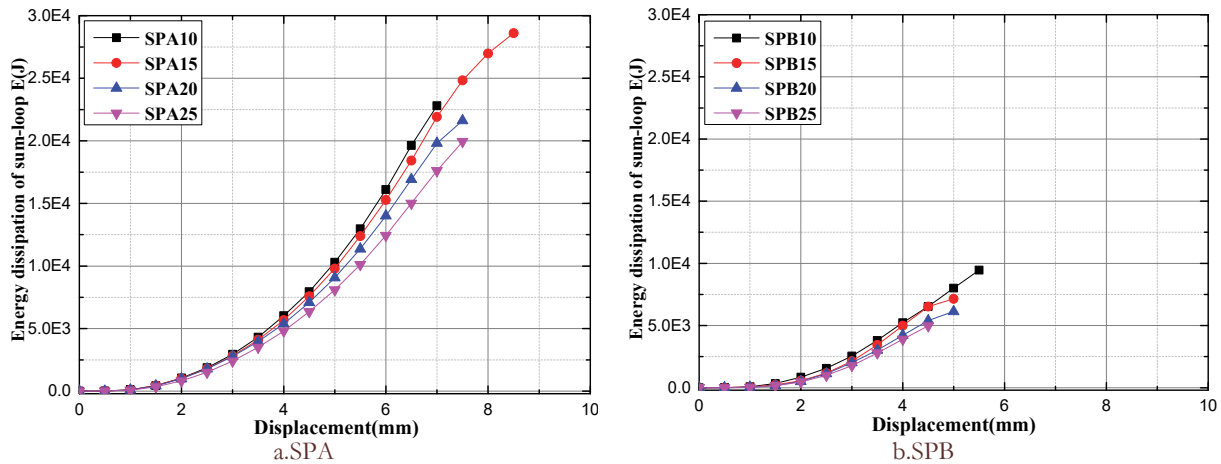

Figure 8: Dissipation capacity comparison of different opening types of dampers with different opening ratios.

Relationship between skeleton hysteresis curve and temperature rise

A big percentage of energy absorbed from outside is dissipated as thermal energy during the irreversible process of fatigue, the amount of heat dissipation during the process is influenced by many factors, such as the load type, stress level, sample size, surface treatment status and surrounding temperatures. Thus the heat dissipation could reflect the energy dissipation during the process of fatigue, in other words, studying the heat dissipation could help study the law of energy dissipation of fatigue.

The thermal energy produced during the deformation of materials is the product accompanied with the evolution of crystal microstructure, and it is not related with the damage revolution process. But the change of temperature field due to heat dissipation could reflect and monitor the evolution process of microstructure flaws and the plastic deformation of crack tip. The amount of heat dissipation could reflect the difference during different damage processes and also reflect the irreversibility of material fatigue damage.

The relationship between the mechanical performance and average temperature rise for dampers with four different opening ratios is shown in Fig. 9. As shown in the figure, the temperature field for the sample was taken by the Infrared camera at the peak load displacement of 1mm and 6mm, the inflection point of temperature rise almost corresponds to the yield point of skeleton hysteresis curve, which indicates that the heat energy during the elastic period is much less while the temperature rise increases suddenly after the yield point and would keep increasing during the stiffness degeneration period. Also the local temperature rise is much higher with higher opening ratio for the same displacement load. For the specific dampers, the highest local temperature rise locates near the holding position of the sample for SPA10 and SPA15, while SPA20 and SPA25 happens near the openings, which indicates that the local plastic yield is the key to induce the average temperature rise of the whole plate.

Also, the temperature rise of SP10 is less than the three other dampers, and the yield point is not very obvious, which is caused by the warping effect that results in the out-of-plane of the center in the damper during the experiment. This is because there is elastic deformation along the direction perpendicular to the neutral layer, the temperature rise near the sample holding position is much higher than the opening location of the plate, so the local temperature rise was not obvious and the steel damper did not yield yet. The total work due to load provided such energy that caused the out-of-plane and could increase the total hysteresis dissipation energy. The out-of-plane deformation, instead of damage, caused the stiffness degeneration along the loading direction. In contrast, the out-of-plane phenomenon is not very obvious due to large opening ratio, so damage is the main reason that causes stiffness degeneration so as that the temperature rise is higher. The change of thermal energy for the four dampers is shown in Fig. 9, in which Fig. 9a and b shows the thermal dissipation energy and thermal convective energy during the experiment. In Fig.9, the blue line is the temperature signal; the green line is the energy dissipation; the orange line is the bearing capacity; and the pink line is the strength degradation of the different dampers.
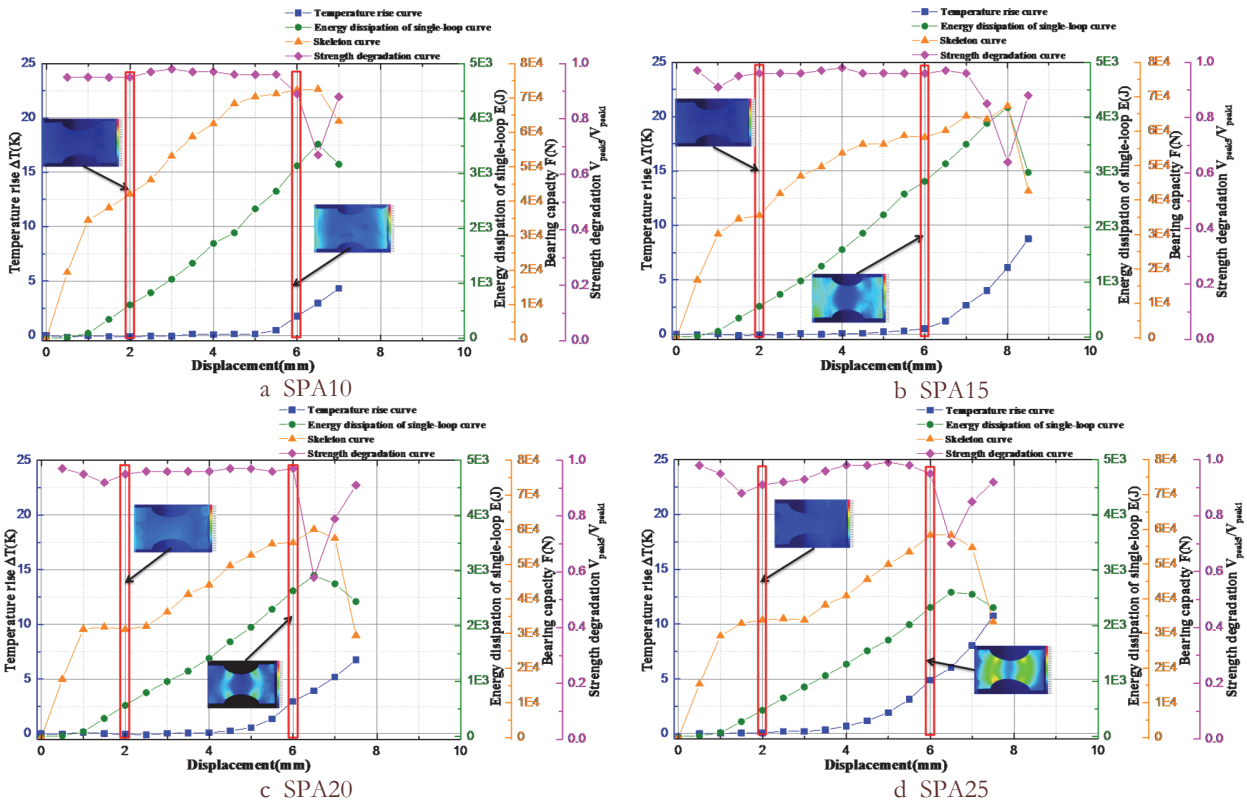
Figure 9: The relationship between the mechanical performance and average temperature rise for dampers of SPA with four different opening ratios.
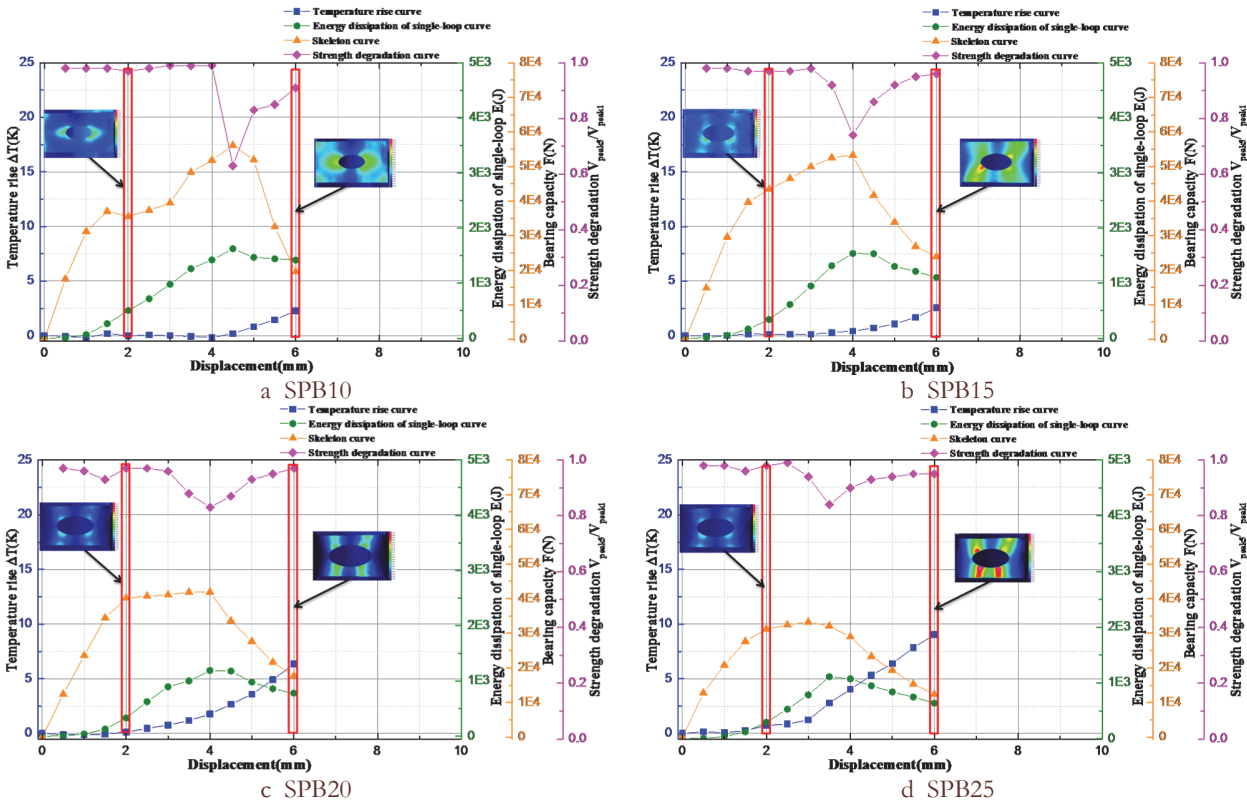

Figure 10: The relationship between the mechanical performance and average temperature rise for dampers of SPB with four different opening ratios.

The thermal energy variation for SPB with different opening ratios during the hysteresis loading process is compared in Fig. 10, in which Fig.10a and Fig. 10b show the thermal dissipation energy based on Heat characterization formula and the thermal convection energy variation trend during the hysteresis process. Similarly, Similarly, In Fig.10, the blue line is the temperature signal; the green line is the energy dissipation; the orange line is the bearing capacity; and the pink line is the strength degradation of the different dampers. From which we could see that the yield point for SPB would appear much earlier than in SPA under the case of same opening ratio. Similarly, the inflection point of temperature rise corresponds with the yielding point of the skeleton curve. Also, the local temperature would have a larger rise as the opening ratio increases under the same maximum displacement load, and the location with larger temperature rise would transfer from two fixture sides to the central opening. And the temperature rise happens earlier for larger opening ratio, and the local stress concentration would induce the obvious improvement of average temperature rise. The hysteresis dissipation energy performance behaves much better with smaller opening ratio, for which the temperature rise is not very obvious even if reaching the yielding point, this is because that the bearing capacity would decrease due to out-of-plane of the specimen instead of local damage. By comparing Fig.9 and Fig. 10, we can see that SPA behaves much better in hysteresis energy dissipation performance than SPB.
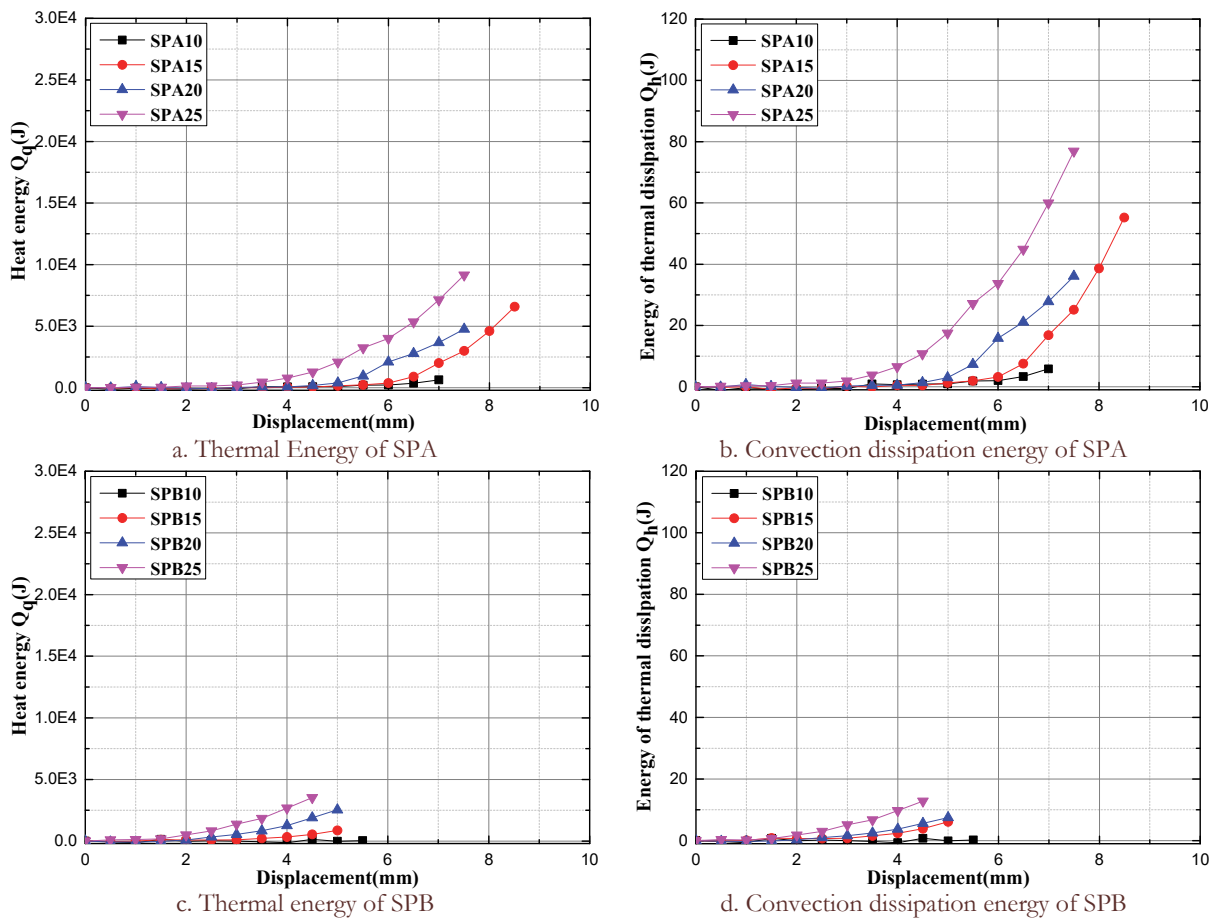

Figure 11: The change of thermal energy during the hysteresis loading.

As shown in Fig.11, the average temperature rise changes earlier and earlier as the opening ratio increases. The thermal energy and convection energy could be calculated according to the temperature rise. The maximum of $\Delta Q(t)$ for SP25 is about 12500J, which holds almost 53% of $\Delta W(t)$. Thus, $\Delta Q(t)$ holds a really significant percentage of $\Delta W(t)$ during the low-cycle hysteresis loading process.

Plastic Energy

Fig.12 shows the plastic damage energy based on the energy conservation law. As can be seen from this figure, the inflection point of thermal dissipation energy would happen earlier as the opening ratio increases, the thermal dissipation

energy and the thermal convection energy is larger and larger as the opening ratio increases with the same displacement load. Also, the thermal energy due to thermal dissipation and convection holds a very large percentage of the total work, which indicates that the thermal energy is very important in plastic deformation and local damage deformation for coupling beam damper during low cycle fatigue test. Moreover, the plastic energy also holds a large part of the total energy. In sum, under the same displacement load, as the opening ratio increases, the bearing capacity and the hysteresis energy would decrease, while the ratio of thermal energy would increase.
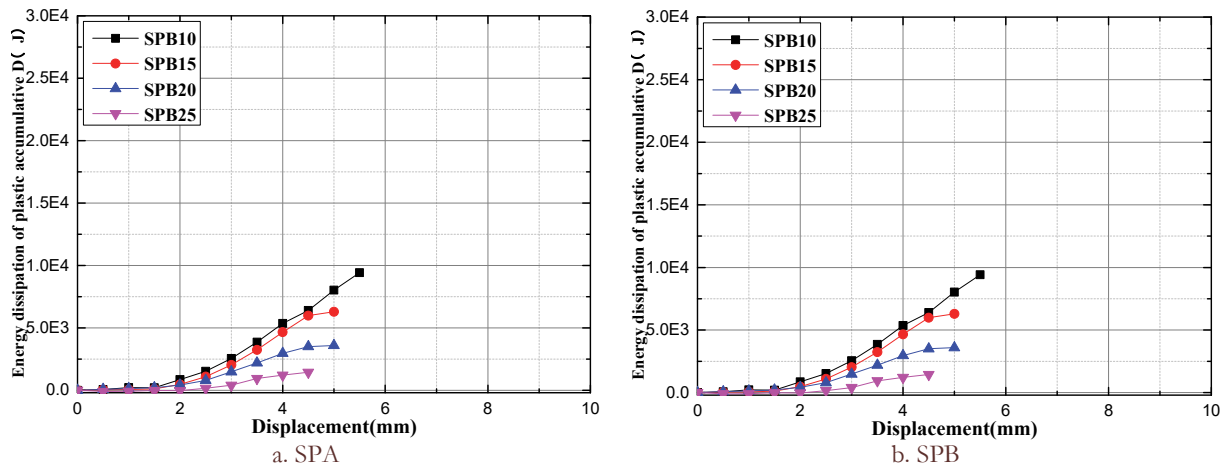
Figure 12: Plastic dissipation energy of SPA and SPB during the cyclic loading process.

CONCLUSION

Based on the traditional hysteresis experiments of metal dampers, and by applying Infrared thermal camera to compare the temperature rise of two different kinds of coupling beam dampers during the experiments. The plastic damage energy and the relationship between different energies could be achieved according to energy balance equation, and the following conclusions could be achieved:

1. Based on the metal damper of SPA, out-of-plane phenomenon would appear easily for smaller opening ratio during the hysteresis process so as to cause the degeneration of stiffness along the loading direction under the case of not obvious yield.
2. With the same opening ratio and same displacement load condition, the hysteresis energy dissipation performance of SPA is much better than SPB.
3. The opening ratio could influence the temperature rise. Specifically, the rapid temperature rise would appear earlier for larger opening ratio.
4. During the hysteresis process of metal beam damper, the thermal energy is produced along the plastic damage and holds a very important part of total energy. The plastic energy is an important factor that deduces fatigue damage and irreversible change of microstructure. A large part of plastic deformation energy would appear in the type of thermal energy so that the temperature rises which in turn reflects microstructure evolution.

ACKNOWLEDGEMENTS

REFERENCES

[1] Paulay, T., Simulated seismic loading of spandrel beams. Journal of the Structural Division, ASCE97 (ST9) (1971)

2407-2419.

[2] Choo, B.S., Coull，A., Stiffening of laterally loaded coupled shear walls on elastic foundations, Building and Environment, 4(19) (1984) 251-256.

[3] Chung, H. S.， Moon, B. W.， Lee, S. K.， Seismic performance of friction dampers using flexure of RC shear wall system, Structural Design of Tall & Special Buildings, 18(7) (2009) 807-822.

[4] Rassati, G. A.， Fortney, P. J， Shahrooz, B. M., Performance evaluation of innovative hybrid coupled core wall systems, American Society of Civil Engineers，(396) (2011) 479-492.

[5] Fortney, P. J., Shahrooz, B. M., Rassati, G. A., The next generation of coupling beams, Composite Construction in Steel and Concrete, V. ASCE (2014) 619-630.

[6] Kim, H. J.， Choi, K. S.， Oh, S. H.， Comparative study on seismic performance of conventional RC coupling beams and hybrid energy dissipative coupling beams used for RC shear walls, 15WCEE， Lisbon， Portugal, (2012) 2254.

[7] Oh, S. H.， Choi, K. Y.， Kim, H. J., Experimental validation on dynamic response of RC shear wall systems coupled with hybrid energy dissipative devices, 15WCEE， Lisbon， Portugal, (2012) 1422.

[8] Mao, C.， Dong, J.， Li, H.， Seismic performance of RC shear wall structure with novel shape memory alloy dampers in coupling beams, Society of Photo-Optical Instrumentation Engineers (SPIE) Conference Series, (2012) 304-320.

[9] Li D, Zhang S, Yang W, Zhang W. Corrosion monitoring and evaluation of reinforced concrete structures utilizing the ultrasonic guided wave technique. International Journal of Distributed Sensor Networks, 10(2) (2014) 827130.

[10] La Rosa, G., Risitano, A., Thermographic methodology for the rapid determination of the fatigue limit of materials and mechanical components, International Journal of Fatigue, 22 (2000) 65-73.

[11] Junling, F., Qiang, G., Yanguang, Z., Stress analysis and fatigue behavior assessment of components with defect based on FEM and Lock-in thermography, Journal of Materials Engineering (8) (2015) 62-71. (in Chinese)

[12] Todhunter, I., Pearson, K., History of the theory of elasticity and of the strength of materials, Cambridge: Cambridge University Press, (1886) 291-364.

[13] Dulieu-Barton, J. M., Stanley, P., Development and applications of thermoelastic stress analysis, The Journal of Strain Analysis for Engineering Design, 33(2) (1998) 93-104.

[14] Inglis, N. P., Hysteresis and fatigue of Wohler rotating cantilever specimen, The Metallurgist, 1(1) (1927) 23-27.

[15] Luong, M. P., Fatigue limit evaluation of metals using an infrared thermographic method, Mechanics of Materials, 28(1-4) (1998) 155-163

[16] Fargione, G., Geraci, A., La Rosa, G., Rapid determination of the fatigue curve by the thermographic method [J]. International Journal of Fatigue, 24(1) (2002) 11-19.

[17] Curà, F., Curti, G., Sesana R. A new iteration method for the thermographic determination of fatigue limit in steels. International Journal of Fatigue, 27(4) (2005) 453-459.

[18] Junling, F., Xinglin, G., Yanguang, Z., Predictions of S-N curve and residual life of welded joints by quantitative thermographic method, Journal of Materials Engineering, (12) (2011) 29-33. (in Chinese).

[19] Junling, F., Xinglin, G., Chengwei, W., Effect of heat treatments on fatigue properties of FV520B steel using infrared thermography, Chinese Journal of Materials Research, 26(1) (2012) 61-67. (in Chinese).

[20] Zhang Z, Ou J, Li D, Zhang S. Optimization Design of Coupling Beam Metal Damper in Shear Wall Structures. Applied Sciences. 7(2) (2017) 137.

[21] Carlomagno, G. M., Berardi, P. G., Unsteady thermotopography in non-destructive testing, C. Warren, ed. Proceedings of the III infrared Information Exchange, St. Louis/ USA.